

Cathode Properties of Na₃MP0₄CO₃ (M = Co/Ni) Prepared by a Hydrothermal Method for Na-ion Batteries

Xie, Baowei

Interdisciplinary Graduate School of Engineering Sciences, Kyushu University

Kitajou, Ayuko

Organization for Research Initiatives, Yamaguchi University

Okada, Shigeto

Institute of Materials Chemistry and Engineering, Kyushu University

Kobayashi, Wataru

Tosoh Corporation

他

<https://doi.org/10.5109/2547345>

出版情報 : Evergreen. 6 (4), pp.262-266, 2019-12. 九州大学グリーンテクノロジー研究教育センター
バージョン :

権利関係 : Creative Commons Attribution-NonCommercial 4.0 International

Cathode Properties of $\text{Na}_3\text{MPO}_4\text{CO}_3$ ($\text{M} = \text{Co/Ni}$) Prepared by a Hydrothermal Method for Na-ion Batteries

Baowei Xie¹, Ayuko Kitajou², Shigeto Okada^{3*}, Wataru Kobayashi⁴,
Masaki Okada⁴, Toshiya Takahara⁴

¹Interdisciplinary Graduate School of Engineering Science, Kyushu University,
6-1, Kasuga Koen, Kasuga, 816-8580, Japan

²Organization for Research Initiatives, Yamaguchi University,
2-16-1 Tokiwadai, Ube 755-8611, Japan

³Institute of Materials Chemistry and Engineering, Kyushu University,
6-1, Kasuga Koen, Kasuga, 816-8580, Japan

⁴Tosoh Corporation, 3-8-2, Shiba, Minato-Ku, 105-0014, Tokyo, Japan

* Corresponding author: E-mail: s-okada@cm.kyushu-u.ac.jp

(Received November 18, 2019; Revised December 25, 2019; accepted December 25, 2019).

Na-ion batteries are considered as next-generation battery technology in light of the abundant and low cost of sodium. Carbonophosphate compounds of $\text{Na}_3\text{MPO}_4\text{CO}_3$ ($\text{M} = \text{Co/Ni}$) with a large theoretical capacity of 191 mAh/g were successfully synthesized by the hydrothermal method and their cathode properties were evaluated in Na-ion batteries for the first time. After high-speed ball milling with acetylene black at 400 rpm for 4 h, $\text{Na}_3\text{CoPO}_4\text{CO}_3$ delivered a better initial capacity, 70 mAh/g. For $\text{Na}_3\text{NiPO}_4\text{CO}_3$, electrochemical performance was not improved even after high-speed ball milling.

Keywords: Na-ion battery; Carbonophosphate; Hydrothermal method

1. Introduction

After their commercialization, lithium ion batteries (LIBs) have been widely used as energy storage system for portable devices and electric vehicles. However, due to the insufficient abundance of Li and minor metals in the earth's crust, LIBs are believed to be too expensive for large-scale grid battery systems. Na-ion batteries (NIBs), having an operating mechanism similar to that of LIBs, are considered a next-generation battery technology¹⁻⁶. Thanks to the abundance of sodium, NIBs have drawn much interest as a low-cost, and low-environmental impact power source. Among the cathode materials used for NIBs, polyanionic compounds⁷⁻¹³ are more promising for energy storage systems in terms of operation voltage, structural stability, and safety compared with layered oxides cathodes¹⁴⁻¹⁹, which release oxygen easily by charging. Recently, the thermodynamically stable carbonophosphate $\text{Na}_3\text{MPO}_4\text{CO}_3$ ($\text{M} = \text{Fe/Mn/Co/Ni}$), which was predicted by ab initio computations, has attracted a lot of attention as a promising cathode for NIBs due to its large theoretical capacity of 191 mAh/g²⁰. $\text{Na}_3\text{MnPO}_4\text{CO}_3$ and $\text{Na}_3\text{FePO}_4\text{CO}_3$ were experimentally synthesized by a hydrothermal method²¹⁻²⁴, and they achieved a discharge capacity of 125 mAh/g and 121

mAh/g under reversible intercalation and deintercalation reactions, respectively^{25,26}.

In this study, we used a hydrothermal method to synthesize $\text{Na}_3\text{MPO}_4\text{CO}_3$ ($\text{M} = \text{Co/Ni}$) and investigated its cathode properties in Na-ion batteries for the first time. We also explored ball milling's effect on the electrochemical performance.

2. Experimental

$\text{Na}_3\text{MPO}_4\text{CO}_3$ ($\text{M} = \text{Co/Ni}$) was synthesized by the hydrothermal method. First, 0.002 mol $\text{Co}(\text{NO}_3)_2 \cdot 6\text{H}_2\text{O}$ (Wako Pure Chemical Industries) as cobalt source was dissolved into 5 ml DI (deionized water) to form a solution A. Second, 0.002 mol $(\text{NH}_4)_2\text{HPO}_4$ (Wako Pure Chemical Industries) as phosphate source and 2 g Na_2CO_3 (Kishida Chemical) as sodium and carbonate sources were dissolved in 10 ml DI to form a solution B. Third, solution A was mixed with solution B under magnetic stirring and transferred to an autoclave, which was then heated in an oven at 120 °C for 20 h. After decreasing operating temperature to 25 °C slowly, the final product was washed by DI and methanol three times and then dried at 40 °C for 12 h. The obtained product of $\text{Na}_3\text{CoPO}_4\text{CO}_3$ was denoted as NCPC. For the synthesis of $\text{Na}_3\text{NiPO}_4\text{CO}_3$, all

the steps were the same as those for NCPC except that $\text{Ni}(\text{NO}_3)_2 \cdot 6\text{H}_2\text{O}$ was used as the starting material. The obtained product of $\text{Na}_3\text{NiPO}_4\text{CO}_3$ was denoted as NNPC. An easy carbon-coating was carried out to improve the electron conductivity. The obtained NCPC or NNPC was ball milled with AB (acetylene black; Denka) by the weight ratio of 60:30 (wt%) at 200 rpm for 0.5 h in an Ar-filled container. For comparison, a high-speed ball milling at 400 rpm for 4 h was also carried out. The obtained NCPC or NNPC was ball milled with AB by a weight ratio of 60:30 (wt%), at 400 rpm for 4 h in an Ar-filled container. Scanning electron microscopy (SEM) was used to confirm the particle size and morphology of NCPC and NNPC using a JSM-6340F JEOL. X-ray diffraction (XRD) was used to characterize the structure of the final products with a scan speed of $2^\circ/\text{min}$ using a Rigaku TTRIII. The obtained samples were mixed with binder of PTFE (Daikin Industries) at a weight ratio of 90:10 (wt%). Subsequently they were punched into pellets (ca. 30 mg cm^{-2} weight loading), which then dried at 120°C 12 h under vacuum. The electrochemical performance of the obtained sample was evaluated using coin cells (CR 2032) and coin cells were assembled in an Ar-filled glove box. 1 M $\text{NaPF}_6/\text{EC}(\text{ethylene carbonate})/\text{DMC}(\text{dimethyl carbonate})$ (1:1 v/v) solution (Tomiyama Pure Chemical Industries) was used as an electrolyte and Na metal (Sigma Aldrich) was used as the anode.

3. Results and Discussion

XRD results and photos of $\text{Na}_3\text{CoPO}_4\text{CO}_3$ and $\text{Na}_3\text{NiPO}_4\text{CO}_3$ synthesized by the hydrothermal method are shown in Figure 1 and Figure 2. The peaks of obtained samples fit well with the calculated patterns based on the standard CIF cards of $\text{Na}_3\text{CoPO}_4\text{CO}_3$ and $\text{Na}_3\text{NiPO}_4\text{CO}_3$ with the space group $\text{P2}_1/\text{m}$ in the literature²⁰. No peaks from impurities were observed. The colors of the final products were purple and light yellow, respectively. As mentioned in the literature²⁵, due to the low ionic and electronic conductivity, high-speed ball milling process is a key step to improving electrochemical performance of the carbonophosphate compound. After the treatment of ball milling, the contact area between cathode and electrolyte solution was enhanced by decreasing the particle size of cathode, which could significantly improve cathode properties. Therefore, we also investigated ball milling effect on the structure of the carbonophosphate compound. The XRD patterns of $\text{Na}_3\text{CoPO}_4\text{CO}_3$ after ball milling with AB at 200 rpm for 0.5 h and 400 rpm for 4 h are shown in Figure 1 (b - c). No obvious changes in the peaks were detected, and the intensities of the obtained samples decreased, indicating the formation of small particles during ball milling. The sample of $\text{Na}_3\text{NiPO}_4\text{CO}_3$ after ball milling also showed the same changes in XRD patterns.

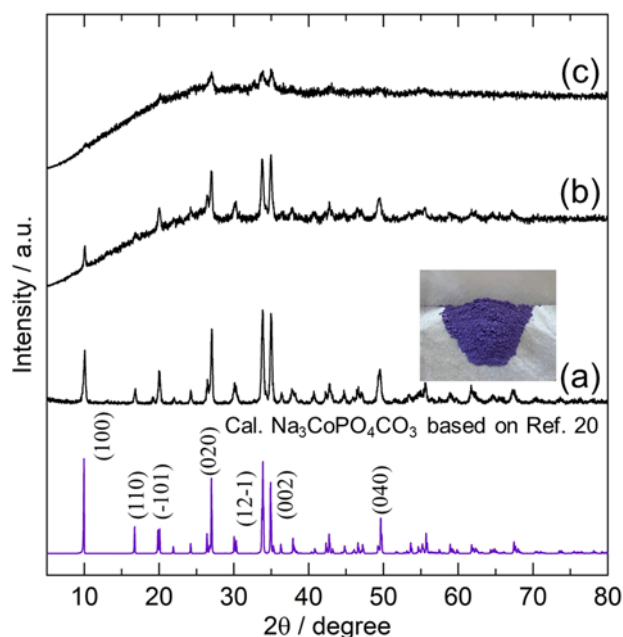


Fig. 1: XRD patterns and photo images (insets) of $\text{Na}_3\text{CoPO}_4\text{CO}_3$ as-synthesized (a); after ball milling with AB at 200 rpm for 0.5 h (b); after ball milling with AB at 400 rpm for 4 h (c).

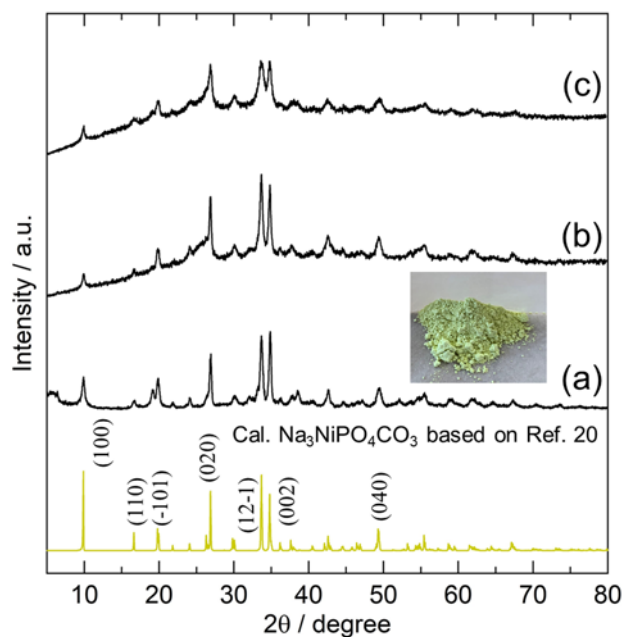


Fig. 2: XRD patterns and photo images (insets) of $\text{Na}_3\text{NiPO}_4\text{CO}_3$ as-synthesized (a); after ball milling with AB at 200 rpm for 0.5 h (b); after ball milling with AB at 400 rpm for 4 h (c).

Figure 3 and Figure 4 show SEM images of $\text{Na}_3\text{CoPO}_4\text{CO}_3$ and $\text{Na}_3\text{NiPO}_4\text{CO}_3$ as-synthesized after balling milling with AB at 200 rpm for 0.5 h and 400 rpm for 4 h, respectively. Before ball milling, agglomeration was observed in both samples, and the particles were about $\sim 100 \mu\text{m}$ (Figure 3 (a) and Figure 4 (a)). After ball milling at 200 rpm for 0.5 h, the particle size was reduced to $\sim 50 \mu\text{m}$ (Figure 3 (b) and Figure 4 (b)). Furthermore, after ball milling at 400 rpm for 4 h, samples had more

irregular morphology and were smaller, $\sim 10\ \mu\text{m}$ (Figure 3 (c) and Figure 4 (c)). The electrochemical performance of the as-synthesized sample after 400 rpm for 4 h was expected to have a better result.

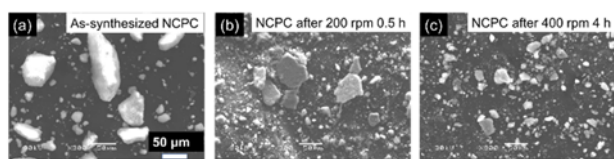


Fig. 3: SEM images of $\text{Na}_3\text{CoPO}_4\text{CO}_3$ as-synthesized (a); after ball milling with AB at 200 rpm for 0.5 h (b); after ball milling with AB at 400 rpm for 4 h (c).

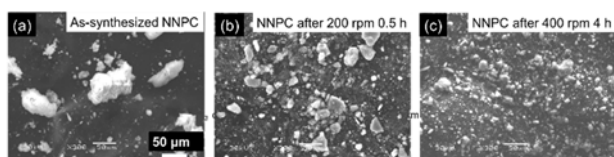


Fig. 4: SEM images of $\text{Na}_3\text{NiPO}_4\text{CO}_3$ as-synthesized (a); after ball milling with AB at 200 rpm for 0.5 h (b); after ball milling with AB at 400 rpm for 4 h (c).

Initial charge-discharge curves of $\text{Na}_3\text{CoPO}_4\text{CO}_3$ and $\text{Na}_3\text{NiPO}_4\text{CO}_3$ investigated between 1.5 - 4.5 V at $0.4\ \text{mA}/\text{cm}^2$ with are shown in Figure 5 and Figure 6. $\text{Na}_3\text{CoPO}_4\text{CO}_3$ ball milled with AB at 200 rpm for 0.5 h delivered a small charge capacity of $74\ \text{mAh}/\text{g}$ and a poor discharge capacity of $30\ \text{mAh}/\text{g}$ at the first cycle (Figure 5 (a)), due to a large overvoltage. However, the samples after ball milling with AB at 400 rpm for 4 h delivered a larger charge capacity of $163\ \text{mAh}/\text{g}$ and a better discharge capacity of $70\ \text{mAh}/\text{g}$ due to the smaller particle size, which increased the contact area among the cathode, the AB, and the electrolyte (Figure 5 (b)). The decrease in particle size confirmed in the SEM images in Figure 3. In addition, two plateaus, which may be associated with the redox pair of $\text{Co}^{2+}/\text{Co}^{3+}$ and $\text{Co}^{3+}/\text{Co}^{4+}$, became more obvious at the first cycle. This indicated that high-speed ball milling activated the electrochemical performance of $\text{Na}_3\text{CoPO}_4\text{CO}_3$, which was similar to that of $\text{Na}_3\text{MnPO}_4\text{CO}_3$ reported in the literature²⁵⁾. The cyclability of NCPC after 15 cycles was summarized in Figure 5 (c). For the samples ball milled with AB at 400 rpm for 4 h and at 200 rpm for 0.5 h, the retention capacity was $45\ \text{mAh}/\text{g}$, and $10\ \text{mAh}/\text{g}$, respectively. For $\text{Na}_3\text{NiPO}_4\text{CO}_3$, the sample ball milled with AB at 200 rpm for 0.5 h delivered a first charge and discharge capacity of $28\ \text{mAh}/\text{g}$ and $10\ \text{mAh}/\text{g}$, respectively (Figure 6 (a)). Even after a high-speed ball milling, the initial charge and discharge capacity increased only to $70\ \text{mAh}/\text{g}$ and $29\ \text{mAh}/\text{g}$, respectively (Figure 6 (b)). As a result, the retention capacity of $\text{Na}_3\text{NiPO}_4\text{CO}_3$ with and without high-speed ball milling were $16\ \text{mAh}/\text{g}$ and $5\ \text{mAh}/\text{g}$ after 15 cycles, respectively (Figure 6 (c)). This may be associated with the higher theoretical operation voltage of Ni-based cathode materials, which could be larger than the

electrochemical potential window of 1 M $\text{NaPF}_6/\text{EC}:\text{DMC}$ (1:1 v/v). The operation voltage of $\text{Li}_3\text{NiPO}_4\text{CO}_3$, having a structure similar to that of the sodium compound of $\text{Na}_3\text{NiPO}_4\text{CO}_3$, was 4.8 V/4.8 V as calculated by density functional theory (DFT)²⁷⁾. For Co-based and Mn-based cathodes, $\text{Li}_3\text{CoPO}_4\text{CO}_3$ and $\text{Li}_3\text{MnPO}_4\text{CO}_3$ had lower voltages of 4.1 V/ 4.6 V and 3.3 V/4.1 V respectively²⁷⁾.

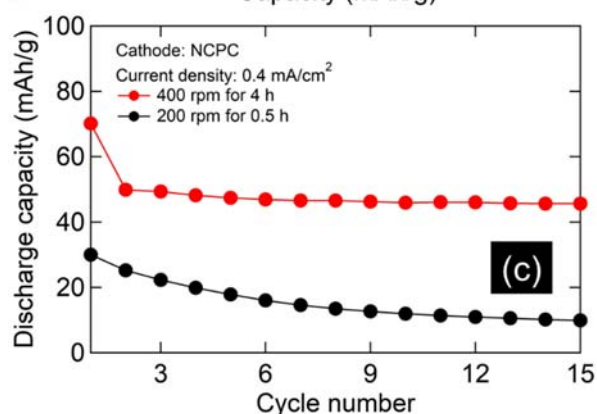
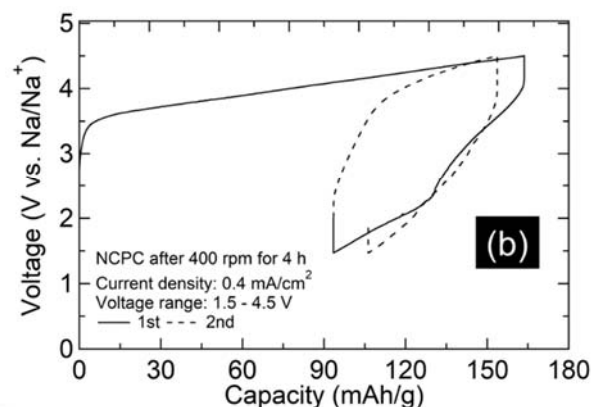
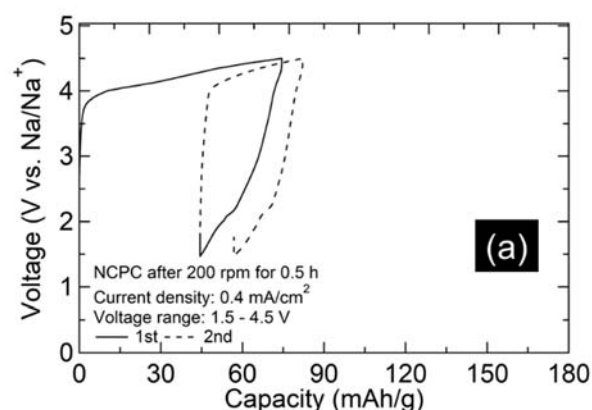


Fig. 5: Initial charge-discharge curves of $\text{Na}_3\text{CoPO}_4\text{CO}_3$ after ball milling with AB at 200 rpm for 0.5 h (a); after ball milling with AB at 400 rpm for 4 h (b); cyclability after 15 cycles (c).

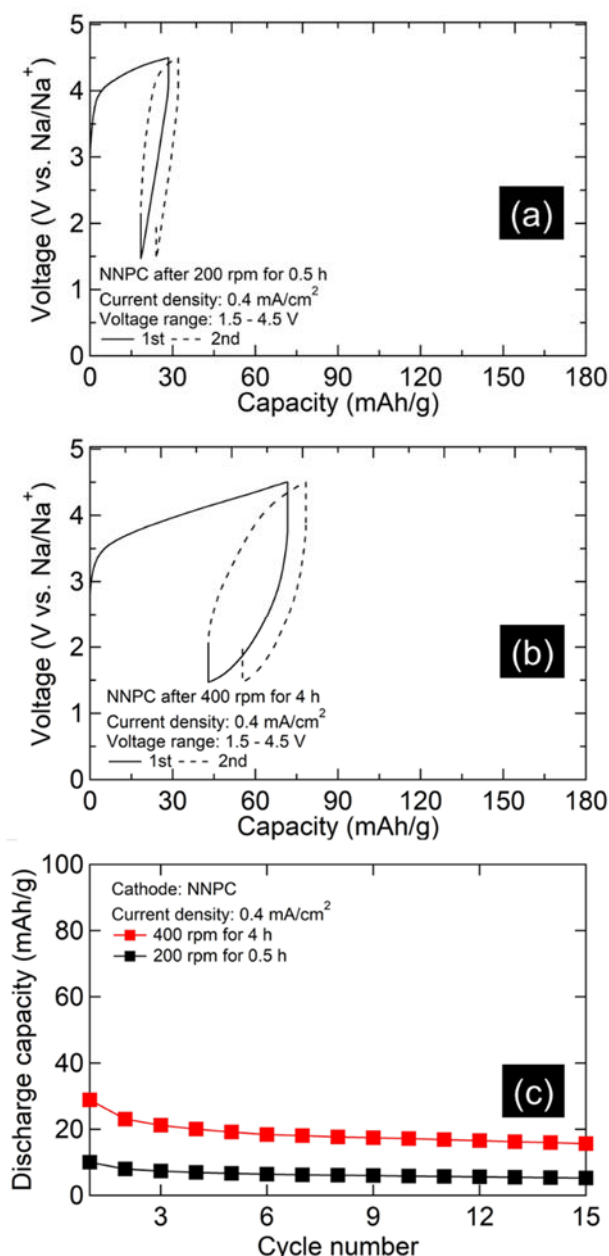


Fig. 6: Initial charge-discharge curves of Na₃NiPO₄CO₃ after ball milling with AB at 200 rpm for 0.5 h (a); after ball milling with AB at 400 rpm for 4 h (b); cyclability after 15 cycles (c).

4. Conclusions

We successfully synthesized the carbonophosphate compounds of Na₃CoPO₄CO₃ and Na₃NiPO₄CO₃ by a hydrothermal method. For the first time, the cathode properties of these compounds were evaluated for Na-ion batteries. For Na₃CoPO₄CO₃, the first discharge capacity was improved from 30 mAh/g to 70 mAh/g after high-speed ball milling with AB at 400 rpm for 4 h, due to the reduction in particle size. However, for Na₃NiPO₄CO₃, high-speed ball milling did not improve the cathode properties. This result may be associated with this compound's high theoretical operation voltage. The electrochemical performance of Na₃NiPO₄CO₃ could be

activated with a new electrolyte with a wide electrochemical potential window.

Acknowledgements

This work was financially supported by the Elements Strategy Initiative for Catalysts and Batteries Project of MEXT, Japan.

References

- 1) S. Komaba, N. Yabuuchi, T. Nakayama, A. Ogata, T. Ishikawa, and I. Nakai, "Study on the Reversible Electrode Reaction of Na_{1-x}Ni_{0.5}Mn_{0.5}O₂ for a Rechargeable Sodium-Ion Battery," *Inorg. Chem.*, **51** (11) 6211–6220 (2012). doi:10.1021/ic300357d.
- 2) Y. Jiang, S. Yu, B. Wang, Y. Li, W. Sun, Y. Lu, M. Yan, S. Song, and S. Dou, "Prussian Blue@C Composite as an Ultrahigh-Rate and Long-Life Sodium-Ion Battery Cathode," *Adv. Funct. Mater.*, **26** (29) 5315–5321 (2016). doi:10.1002/adfm.201600747.
- 3) Y. Xu, Q. Wei, C. Xu, Q. Li, Q. An, P. Zhang, J. Sheng, L. Zhou, and L. Mai, "Layer-by-layer Na₃V₂(PO₄)₃ embedded in reduced graphene oxide as superior rate and ultralong-life sodium-ion battery cathode," *Adv. Energy Mater.*, **6** (14) 1600389–1600398 (2016). doi:10.1002/aenm.201600389.
- 4) Q. Zhang, W. Wang, Y. Wang, P. Feng, K. Wang, S. Cheng, and K. Jiang, "Controllable construction of 3d-skeleton-carbon coated Na₃V₂(PO₄)₃ for high-performance sodium ion battery cathode," *Nano Energy*, **20** 11–19 (2016). doi:10.1016/j.nanoen.2015.12.005.
- 5) K. Nakamoto, R. Sakamoto, A. Kitajou, M. Ito, and S. Okada, "Cathode properties of sodium manganese hexacyanoferrate in aqueous electrolyte," *Evergreen*, **4** (1) 6–9 (2017). doi:10.5109/1808305.
- 6) K. Chihara, M. Ito, A. Kitajou, and S. Okada, "Cathode property of Na₂C_xO_x [x = 4, 5, and 6] and K₂C₆O₆ for sodium-ion batteries," *Evergreen* **4** (1) 1–5 (2017). doi:10.5109/1808304.
- 7) N. Yabuuchi, K. Kubota, M. Dahbi, and S. Komaba, "Research development on sodium-ion batteries," *Chem. Rev.*, **114** (23) 11636–11682 (2014). doi:10.1021/cr500192f.
- 8) J. Lu, S. Nishimura, and A. Yamada, "Polyanionic Solid-Solution Cathodes for Rechargeable Batteries," *Chem. Mater.*, **29** (8) 3597–3602 (2017). doi:10.1021/acs.chemmater.7b00226.
- 9) A. Inoishi, T. Omuta, E. Kobayashi, A. Kitajou, and S. Okada, "A Single-Phase, All-Solid-State Sodium Battery Using Na_{3-x}V_{2-x}Zr_x(PO₄)₃ as the Cathode, Anode, and Electrolyte," *Adv. Mater. Interfaces*, **4** (5) 1600942–1600947 (2017). doi:10.1002/admi.201600942.
- 10) A. Inoishi, Y. Yoshioka, L. Zhao, A. Kitajou, and S. Okada, "Improvement in the Energy Density of

- $\text{Na}_3\text{V}_2(\text{PO}_4)_3$ by Mg Substitution,” *ChemElectroChem*, **4** (11) 2755–2759 (2017). doi:10.1002/celec.201700540.
- 11) K. Chayambuka, G. Mulder, D.L. Danilov, and P.H.L. Notten, “Sodium-Ion Battery Materials and Electrochemical Properties Reviewed,” *Adv. Energy Mater.*, **8**, (16) 1800079–1800128 (2018). doi:10.1002/aenm.201800079.
 - 12) R. Liu, Z. Liang, Z. Gong, and Y. Yang, “Research Progress in Multielectron Reactions in Polyanionic Materials for Sodium-Ion Batteries,” *Small Methods*, **3** (4) 1800221–1800243 (2019). doi:10.1002/smt.201800221.
 - 13) A. Kitajou, H. Momida, T. Yamashita, T. Oguchi, and S. Okada, “Amorphous $x\text{NaF-FeSO}_4$ Systems ($1 \leq x \leq 2$) with Excellent Cathode Properties for Sodium-Ion Batteries,” *ACS Appl. Energy Mater.*, **2** (8) 5968–5974 (2019). doi:10.1021/acsaem.9b01053.
 - 14) R.J. Clément, P.G. Bruce, and C.P. Grey, “Review-Manganese-Based P2-Type Transition Metal Oxides as Sodium-Ion Battery Cathode Materials,” *J. Electrochem. Soc.*, **162** (14) A2589–A2604 (2015). doi:10.1149/2.0201514jes.
 - 15) D. Yuan, X. Hu, J. Qian, F. Pei, F. Wu, R. Mao, X. Ai, H. Yang, and Y. Cao, “P2-type $\text{Na}_{0.67}\text{Mn}_{0.65}\text{Fe}_{0.2}\text{Ni}_{0.15}\text{O}_2$ Cathode Material with High-capacity for Sodium-ion Battery,” *Electrochim. Acta*, **116** 300–305 (2014). doi:10.1016/j.electacta.2013.10.211.
 - 16) J. Zhao, L. Zhao, N. Dimov, S. Okada, and T. Nishida, “Electrochemical and Thermal Properties of $\alpha\text{-NaFeO}_2$ Cathode for Na-Ion Batteries,” *J. Electrochem. Soc.*, **160** (5) A3077–A3081 (2013). doi:10.1149/2.007305jes.
 - 17) P.F. Wang, Y. You, Y.X. Yin, and Y.G. Guo, “Layered Oxide Cathodes for Sodium-Ion Batteries: Phase Transition, Air Stability, and Performance,” *Adv. Energy Mater.*, **8** (8) 1701912–1701935 (2018). doi:10.1002/aenm.201701912.
 - 18) X. Xiang, K. Zhang, and J. Chen, “Recent Advances and Prospects of Cathode Materials for Sodium-Ion Batteries,” *Adv. Mater.*, **27** (36) 5343–5364 (2015). doi:10.1002/adma.201501527.
 - 19) M.H. Han, E. Gonzalo, G. Singh, and T. Rojo, “A comprehensive review of sodium layered oxides: powerful cathodes for Na-ion batteries,” *Energy Environ. Sci.*, **8** (1) 81–102 (2015). doi:10.1039/c4ee03192j.
 - 20) H. Chen, G. Hautier, and G. Ceder, “Synthesis, computed stability, and crystal structure of a new family of inorganic compounds: carbonophosphates,” *J. Am. Chem. Soc.*, **134** (48) 19619–19627 (2012). doi:10.1021/ja3040834.
 - 21) C. Wang, M. Sawicki, J.A. Kaduk, and L.L. Shawa, “Roles of processing, structural defects and ionic conductivity in the electrochemical performance of $\text{Na}_3\text{MnCO}_3\text{PO}_4$ cathode material,” *J. Electrochem. Soc.*, **162** (8) A1601–A1609 (2015). doi:10.1149/2.0801508jes.
 - 22) C. Wang, M. Sawicki, S. Emani, C. Liu, and L.L. Shaw, “ $\text{Na}_3\text{MnCO}_3\text{PO}_4$ – A High Capacity, Multi-Electron Transfer Redox Cathode Material for Sodium Ion Batteries,” *Electrochim. Acta*, **161** 322–328 (2015). doi:10.1016/j.electacta.2015.02.125.
 - 23) N. Hassanzadeh, S.K. Sadrezaad, and G. Chen, “In-situ hydrothermal synthesis of $\text{Na}_3\text{MnCO}_3\text{PO}_4/\text{rGO}$ hybrid as a cathode for Na-ion battery,” *Electrochim. Acta*, **208** 188–194 (2016). doi:10.1016/j.electacta.2016.05.028.
 - 24) N. Kosova, A. Shidrov, A. Slobodyuk, and D. Kellerman, “Thermal and structural instability of sodium-iron carbonophosphate ball milled with carbon,” *Electrochim. Acta*, **302** 119–129 (2019). doi:10.1016/j.electacta.2019.02.001.
 - 25) H. Chen, Q. Hao, O. Zivkovic, G. Hautier, L. Du, Y. Tang, Y. Han, X. Ma, C. Grey, and G. Ceder, “Sidorenkite ($\text{Na}_3\text{MnPO}_4\text{CO}_3$): a new intercalation cathode material for Na-ion batteries,” *Chem. Mater.*, **25** (14) 2777–2786 (2013). doi:10.1021/cm400805q.
 - 26) W. Huang, J. Zhou, B. Li, J. Ma, S. Tao, D. Xia, W. Chu, and Z. Wu, “Detailed investigation of $\text{Na}_{2.24}\text{FePO}_4\text{CO}_3$ as a cathode material for Na-ion batteries,” *Sci. Rep.*, **4** 4188–4196 (2014). doi:10.1038/srep04188.
 - 27) G. Hautier, A. Jain, H. Chen, C. Moore, S.P. Ong, and G. Ceder, “Novel mixed polyanions lithium-ion battery cathode materials predicted by high-throughput ab initio computations,” *J. Mater. Chem.*, **21** (43) 17147–17153 (2011). doi:10.1039/c1jm12216a.